

## Manufacturing and Performance Evaluation of Soy-Based Nanocomposites

by

A. Shabeer, S. Sundararaman, V.G.K. Menta and  
K. Chandrashekara

Department of Mechanical and Aerospace Engineering

T. Schuman

Department of Chemistry  
University of Missouri-Rolla, Rolla, MO 65409

### Abstract

Epoxy-clay nanocomposites were synthesized using a soy-based epoxy resin, which was prepared by the process of transesterification and epoxidation of regular food grade soybean oil. Nanoclay was dispersed into the soy-based epoxy resin using a high shear mixer and sonication. Tensile testing of the nanocomposites showed that the nanoclay improved the modulus and the strength by 625% and 340%, respectively. Exfoliation of the nanoclay was investigated by X-ray diffraction. The influence of the montmorillonite clay upon the curing efficiency of the epoxy-anhydride resin system was studied as a function of the clay concentration using differential scanning calorimetry. Rheological test were also conducted to find the suitability of using the soy-based epoxy clay nanocomposites toward common composite manufacturing applications. The soy-based nanocomposites hold great promise as environmentally friendly and low cost materials for structural applications.

### Introduction

Polymer nanocomposites have become increasingly popular for their improved mechanical, thermal, barrier, electrical, flame retardant, and optical properties [1-2]. Nanocomposites are a relatively new area of materials in which at least one dimension of the dispersed particles is in the nanometer range. Commonly used nanoparticles include colloidal silica, carbon nanotubes, whiskers, and clay platelets [3]. Among the nanoparticles, clay platelets are particularly attractive due to their high performance at low filler loadings, rich intercalation chemistry, high surface area, high strength and stiffness, high aspect ratio

of individual platelets, abundance in nature and especially low cost [4].

The chemical structure of the clay consists of nanometer thick platelets of octahedral aluminum atoms sandwiched as a sheet between two silicon tetrahedron sheets. The dimensions of these silica sheets are approximately 0.96 nm in thickness and approximately 100 to several hundred nanometers in length [5]. The unique layered structure of clay particles and intercalation capabilities allow them to be chemically modified to be compatible with various polymers. Usuki et al. [6] explored the possibility of synthesizing nanocomposites from polyamide and organophilic montmorillonite clay.

The polyamide-clay nanocomposites showed a major improvement in the physicomechanical properties of the composite at very low clay content. Over the years, several researchers have similarly demonstrated the usage of clay particles as reinforcement in nanocomposites based on epoxies, unsaturated polyesters, and polyurethane [7]. A potential drawback of clays is the incompatibility between hydrophilic clay and hydrophobic polymer, which often causes agglomeration of the clay in the polymer matrix. Therefore, surface modification of the clay is an important step in achieving polymer nanocomposites dispersion and performance. For instance, surface modification can be achieved by treating the clay with a long chain alkyl amine so as to make it organophilic.

Three different methods to synthesize polymer-clay nanocomposites are the solution approach, in-situ polymerization, and melt intercalation. In the present study, an in-situ polymerization method is used whereby organoclay is swollen in the pre-polymer resin, then a curing agent is added and nanocomposites are formed. Many attempts have been made to modify clay using organic cations such as ammonium, phosphonium, imidazolium, etc. Chen and Curliss [8] prepared epoxy nanocomposites from a series of organoclays modified with alkyl ammonium chlorides with different length alkyl groups.

Kornmann et al. [9] reported that a long chain alkylamine having a chain of more than eight carbon atoms could result in an exfoliated structure. Wang et al. [10] prepared nanocomposites in which the inorganic cations were replaced by organic ions via ion exchange. This exchange of ions increased the spacing between the silicate layers, which in turn promoted the penetration of polymer chains into the space between layers. Nigam et al. [11] reported that octadecylammonium ions exchanged for Na<sup>+</sup> ions of pristine montmorillonite resulted in exfoliation of clay. They also reduced the Van der Waals interactions between the silicate layers, which

avored penetration of the polymer between these clay layers.

In recent years, polymeric materials prepared from natural and renewable resources such as triglyceride vegetable oils are finding numerous applications. The fatty acid esters derived from the triglyceride vegetable oils are an attractive source of raw materials for polymer synthesis. Among the triglyceride oils, soybean attracts great interest because of its plentiful supply in the United States, relatively low cost and environmentally benign properties. Soybean oil contains 85% unsaturated oleic, linoleic and linolenic fatty acids. This high degree of unsaturation makes it possible to polymerize the oil into useful materials. The carbon-carbon double bonds can be epoxidized to form reactive groups, which are capable of forming a cross-linking polymer network structure.

Several researchers have attempted to use epoxidized soybean oil (ESO) for polymeric and composite applications [12]. However, due to lower reactivity and a tendency to intra-molecular bonding, ESO normally has a low cross-linking density and therefore limited thermal and mechanical properties. Most ESO industrial applications are still limited to nonstructural applications such as coatings and poly vinyl chloride (PVC) additives of low strength requirements. In a previous study, a soy-based epoxy resin system, epoxidized allyl soyate (EAS), was synthesized by the addition of epoxidized soybean oil to the base Shell Epon resin [13-14]. EAS resin has proved to be more flexible and it tends to improve some of the mechanical properties.

In the present work, soy-based epoxy nanocomposites were synthesized using soy-based epoxy resin and montmorillonite clay. The mechanical and rheological properties have been analyzed. The structure of the nanocomposites was investigated by wide angle X-ray diffraction. The curing mechanisms with the different amounts of montmorillonite clay were studied using differential scanning calorimetry.

## Experimental

### Materials

The base epoxy resin used in the study was Shell Epon® 9500 (Shell Chemical Co. Houston, TX). Lindride® LS 56V (Lindau Chemicals, Columbia, SC) was the anhydride curing agent used. Soy-based resin was synthesized in a two-step laboratory scale process from regular food grade soybean oil. At first the triglyceride molecules in the soybean oil were transesterified with allyl alcohol to yield fatty acid allyl esters. Next, the fatty acid esters were epoxidized using benzoyl peroxide to yield soyate epoxy resin. The clay used in this study, Closite® 30B, is commercially

available from Southern Clay Products Inc. (Gonzales, TX), which is a montmorillonite clay modified with a quaternary ammonium salt with an initial interlayer d spacing of 18.5 Å. The cation exchange capacity of the clay is 90meq/100g of clay.

### Preparation of soy-based epoxy/clay nanocomposites

Epoxy-resin blends were prepared by mixing the soy epoxy resin with the base Epon resin. The weight ratio of soy epoxy resin to Epon resin blend chosen for the present work was 75:25 as shown in Table 1. The clay was dried at 60°C for a day under vacuum before sample preparation.

Soy epoxy resin was mixed with the clay in varied proportions of 0, 2.5 and 5 wt% with respect to 100 wt% of the composite using a high speed pneumatic mixer for 30 min followed by 100 W sonication for 5 min. Next, a stoichiometric weight of curing agent was added to the epoxy/clay mixture. The resin and the hardener were mixed well. The composite mixture was degassed in a vacuum oven for few minutes to remove any air bubbles. The mixture was poured into a preheated mold, which had been sprayed with a mold release agent, Chemlease® 41 (Chem-Trend Incorporated, Howell, MI). Curing was performed in the oven in two stages. First, the mixtures were cured for 1 hour at 80°C and then followed by curing for 1.5 hours at 175°C.

### Tensile test

The tensile tests were carried out as per ASTM D 638 on an Instron Universal testing machine. Tensile modulus, tensile strength, and the elongation at break values were evaluated. All the tensile tests were performed at a crosshead speed of 0.5 mm/min. At least five specimens were tested for each different resin system and the average values are reported with corresponding error bars at ±1 standard deviation from the mean.

### X-Ray diffraction analysis

X-ray diffraction (XRD) patterns were obtained using a Scintag XDS 2000 diffractometer equipped with Cu-K $\alpha$  radiation at a wavelength of 0.15418 nm, accelerating voltage of 40 Kv, and electric flow of 100 mA. The scanning range was from 2° to 8° with a rate of 0.01 degree /min. The corrected intensity was smoothed and plotted versus 2 $\theta$ . From the position of a peak, the corresponding d spacing was computed from the Bragg's diffraction equation:

$$n\lambda = 2d \sin \theta,$$

where n is the order of reflection,  $\lambda$  is the wavelength of radiation,  $\theta$  is the angle of reflection and d is the interlamellar spacing.

## Differential scanning calorimetry

Differential scanning calorimetry (DSC) testing was performed on TA Instrument model 2010. The samples of 10-14mg of soy-based epoxy resin-curing agent with 2.5% and 5% of montmorillonite clay were each placed into an aluminum crucible. The curing exotherms were made at a rate of 10° C/min from 30 to 250°C. The onset of cure, heat of reaction, and end of cure was measured for each sample. Once the samples were cured in the DSC, the cell was quickly cooled using liquid nitrogen and subjected to subsequent scanning from -100°C to 150°C to measure the resulting glass transition temperature. The glass transition temperature ( $T_g$ ) was reported as the inflection point of the glass transition region.

## Viscosity measurements

Viscosities of the resins were measured using Brookfield CAP 2000 viscometer, which was equipped with cone and plate geometry. All measurements were conducted at 25°C. Viscosity of the resin was measured by varying the shear rate during the testing. The data were collected and analyzed using CAPCALC software.

## Results and Discussion

### Mechanical characterization

Figure 1 shows the typical tensile stress versus strain trends of the composites as a function of increasing percent loading of the clay. Figure 2 shows the tensile modulus, tensile strength and percent elongation of the nanocomposites with as a function of clay concentration, respectively. With only 2.5wt% of clay added to the soy-based epoxy matrix, the Young's modulus and tensile strength were increased to 13 and 22 MPa, respectively for blends prepared using sonication. The remarkable increases suggested that a nano composite structure had been formed. The role of clay as a reinforcing agent in the nanocomposites was clearly evident from the curves. The observed increase in modulus of the nanocomposites may be ascribed to an increased apparent aspect ratio of the clay, where the effect of the aspect ratio of the filler particle on the modulus can be estimated using Guth's equation [15]. The dependence of the modulus on the volume fraction of the clay can be predicted by taking into account the aspect ratio of the clay and can be expressed as:

$$E_C = E_m (1 + 0.67 f_g v_f + 1.62 f_g^2 v_f^2),$$

where  $E_C$  is the modulus of the composite,  $E_m$  is the modulus of the resin,  $f_g$  is the apparent aspect ratio of clay platelets and  $v_f$  is volume fraction of clay.

The apparent aspect ratios of the clay particles in the nanocomposites are 116 and 60, respectively, for 2.5% clay soy epoxy anhydride polymer and 5% clay soy epoxy anhydride polymer. The decrease in apparent aspect ratio for 5% clay soy epoxy anhydride polymer can be attributed to increased agglomeration of clay particles at the higher loading level. The calculated values of the apparent aspect ratios suggest that the clay is in platelet form.

The nature of the interaction between the base resin and the filler strongly influences peak stress of the nanocomposites. With the initial increase in clay content, the stress to break increased for the nanocomposites, which correlated with the assumption that there existed good interactions between the clay particles and the soy-based epoxy resin. The percent elongation decreased with the increase in concentration of clay. Soy-based epoxy polymer exhibited ductile failure, whereas upon the addition of clay a brittle fracture of the soy-based epoxy composites was observed, as evidenced by minimal or no distinct plastic deformation region. The possible explanation to this phenomenon is the silicate platelets constrain the matrix so that plastic deformations are prevented in the nanocomposites.

### X-ray diffraction analysis

X-ray diffraction is commonly used for the characterization of organo-clay particles in polymer nanocomposites to study the intercalation and exfoliation of layered composites. The interlayer spacing of montmorillonite clay can be calculated from the peak intensity angle of diffraction using the Bragg equation. In intercalated nanocomposites, the interlayer spacing was increased as shown by a shift of the diffraction peak toward a lower angle, whereas for exfoliated nanocomposites, no diffraction peak was observed via XRD. Nanocomposites are formed when there is an increase in gallery spacing evidenced by a decrease in the diffraction angle.

Nonexfoliated montmorillonite clay particles can consist of hundreds of individual layers and the distance between two adjacent layers is called  $d$ -spacing or basal spacing. The layers are approximately 1nm thick and possess high aspect ratios. The  $d$ -spacing corresponding to the (001) peak position for Cloisite 30B used in this study was about 18.5Å. Figure 3 shows the typical XRD pattern of pure clay, and 2.5% and 5% clay in soy epoxy anhydride polymer composites that were mixed using the sonication method. Pure clay showed the characteristic peak at  $2\theta = 4.7^\circ$ , which corresponds to basal spacing of 18.5Å.

In contrast to pure clay, the 2.5% clay soy epoxy anhydride polymer and 5% clay soy epoxy anhydride polymer did not show a distinct clay peak in the  $d$  (001)

spacing region, which seems to indicate exfoliation. The distinct clay peak  $2\theta = 4.7^\circ$  was not observed. Compared to the XRD of pure clay, the (001) peak was not present and did not shift to lower angles, indicating that the clay was exfoliated, i.e. does not show a regular repeat distance between the platelets. One explanation for this phenomenon is that the epoxy anhydride resins readily penetrate into the clay galleries, probably due to interaction between the organo-modified clay hydroxyl and the anhydride of the resin blend. Infrared absorption and DSC evidence supported this hypothesis by demonstrating interaction between the clay and the anhydride group.

The above measurements only indicate that the basal spacing of the clay is higher than 8.8 nm, which is the practical detection limit of the XRD analysis. Since disappearance of the peak corresponding to basal spacing could be due to insufficient signal from low clay concentration, higher percentages of clay were added separately to the soy resin and the neat curing agent and subjected to X-ray diffraction studies.

Figure 4 shows the X-ray diffraction pattern of 10% clay dispersed in uncured soy-Epon mixed using sonication. The diffraction pattern showed basal reflection at  $2\theta = 4.467^\circ$  giving  $d$ -spacings of 1.978nm for 10% clay mixed with ultrasonic. The diffraction peaks shifted toward a lower angle direction for ultrasonic mixed samples indicating some additional expansion of the interlayer distance of the clay. This expansion of the gallery height was attributed to the intercalation of epoxy molecules into the interlayer of the clay. The presence of these peaks in the diffraction pattern was important to our study because it demonstrated that the X-ray analysis was sensitive enough to detect the presence of the layered silicate.

Figure 5 shows the X-ray diffraction pattern of 5% clay dispersed in the anhydride in curing agent alone. The diffraction peak disappeared indicating an exfoliation of clay in the curing agent, and disruption of the natural layered structure. The explanation at this point may be attributed to the reaction of organo modifier in clay and the anhydride curing agent leading to a more facile disruption of the layered structure compared to the epoxy resins. What remained clear from the tensile and XRD analysis was that improved dispersion and exfoliation of clay particles yielded significant improvements in the mechanical properties of the nanocomposites, which was enhanced in the presence of anhydride resin and use of the sonication method of preparation.

### Differential scanning calorimetry

Figure 6 shows the DSC spectra of soy epoxy anhydride polymer, and 2.5% clay and 5% clay in soy

epoxy anhydride polymer composites. Table 2 summarizes the DSC results. The DSC exotherms show that an increase of the clay content caused a shift in the exotherm peak maximum to lower values. The onset temperature of curing and the temperature of the exothermal heat maximum for the neat soy resin were  $79.6^\circ\text{C}$  and  $160.3^\circ\text{C}$ , respectively, whereas they were  $75.7^\circ\text{C}$  and  $157.7^\circ\text{C}$  for the 2.5% clay soy epoxy anhydride polymer composite and  $71.6$  and  $157.2^\circ\text{C}$  for the 5% clay soy epoxy anhydride polymer composite, respectively. This demonstrated that the onset temperature for curing and the temperatures of maximum exotherm heat shifted to lower temperatures for soy epoxy anhydride polymer-clay nanocomposites as compared to soy epoxy anhydride polymer.

It can also be seen that the heat of reaction per gram of the polymer was reduced upon an increase in concentration of clay. Figure 7 shows the glass transition curves of the soy-based nanocomposites. A slight decrease of  $T_g$  with increasing concentration of clay was observed in this study, which is observed for nanomaterials dispersed in polymers [16]

### Viscosity measurements

Rheological measurements were conducted to find the suitability of using the soy-based epoxy clay nanocomposites in composite manufacturing applications. The viscosities of the uncured soy-based epoxy nanocomposites were measured at  $25^\circ\text{C}$  using a Brookfield Cap 2000 viscometer. Figure 8 shows the variation of viscosity with shear rate. The viscosity of soy-based epoxy nanoclay composites increased from 5 to 24 poise with the increase in clay concentration. However, the increase of viscosity was limited and the rheologically processable window is still large for composite manufacturing applications. Thus, the initial test results indicate that the soy-based epoxy clay nanocomposites can be used as base resin in most composite manufacturing applications.

### Conclusion

Nanocomposites of soy-based epoxy resin and an organo modified montmorillonite clay were successfully prepared. The tensile test results showed a substantial increase in the strength and modulus of the composites compared to polymer alone. From the XRD results, it was concluded that the nanoclay was fully exfoliated into the resin due to a clay interaction with the anhydride. DSC plots showed that the addition of clay in the resin shifted the onset of curing to lower temperatures and less exotherm heat, which was consistent with the clay behaving as segregated reaction accelerant. However, the glass transition temperature of the polymer decreased with increasing clay loading for a constant ratio of anhydride to epoxy. This decrease in glass transition

temperature was attributed to a reduced crosslink density of the epoxy polymer due to the presence of nanoclay. Rheological measurements showed that the addition of clay into the resin did not show a significant change in the viscosity of the resin. Improved physical properties for the clay composite make the soy resin more suitable as a polymer matrix in composite manufacturing applications.

## Acknowledgements

This project is sponsored by National Science Foundation (Grant # NSF CMS-0533201). Partial support from the Missouri Soybean Merchandising Council (MSMC) and the University Transportation Center is gratefully acknowledged.

## References

1. Pinnavaia, T.J.; Beall, G.W. "Polymer-clay nanocomposites," Wiley, London 2000.
2. Akelah, A.; Moet, A. "Polymer-clay nanocomposites: Free radical grafting of polystyrene on to organophilic montmorillonite interlayers," *Journal of Materials Science*, Vol. 31, pp. 3589-3596, 1996.
3. Zeng, Q.H.; Yu, A.B.; Lu, G.Q.; Paul, D.R. "Clay-based polymer nanocomposites: Research and commercial development," *Journal of Nanoscience and Nanotechnology*, Vol. 5, pp. 1574-1592, 2005.
4. Blumstein, A. "Polymerization of adsorbed monolayers. I. Preparation of the clay-polymer complex," *Journal of Polymer Science: Part A*, Vol. 3, pp. 2653-2664, 1965.
5. El Harrak, A.; Carrot, G.; Oberdisse, J.; Eychenne-Baron, Ch.; Boue, F.; "Surface -atom transfer radical polymerization from silica nanoparticle with controlled colloidal stability," *Macromolecules*, Vol. 37, pp. 6376-6384, 2004.
6. Usuki, A; Kojima, Y; Kawasumi, M; Okada, A; Fukushima, Y; Kurauchi, T.; Kamigaito, O "Synthesis of nylon 6- clay hybrid," *Journal of Materials Research*, Vol. 8, pp. 1179-1184, 1993.
7. Wang, Z.; Pinnavaia, T.J. "Nanolayer reinforcement of elastomeric polyurethane," *Chemistry of Materials*, Vol. 10, pp. 3769-3771, 1998.
8. Chen, C.; Curliss, D. "The role of preconditioning on morphology development in layered silicate thermoset nanocomposites," *Journal of Applied Polymer Science*, Vol. 90, pp. 2276-2287, 2003.
9. Kornmann, X.; Lindberg, H.; Berglund, L.A. "Synthesis of epoxy-clay nanocomposites: influence of the nature of the clay on structure," *Polymer*, Vol. 42, pp. 1303-1310, 2001.
10. Wang, Z.; Pinnavaia, T.J. "Hybrid organic-inorganic nanocomposites: Exfoliation of nanolayers in an elastomeric epoxy polymer," *Chemistry of Materials*, Vol. 10, pp. 1820-1826, 1998.
11. Nigam, V.; Setua, D.K.; Mathur, G.N.; Kar, K.K. "Epoxy-montmorillonite clay nanocomposites: Synthesis and characterization," *Journal of Applied Polymer Science*, Vol. 93, pp. 2201-2210, 2004.
12. Nevin, C.S.; Moser, B.F. "Vinyl oil Monomer - vicinal methacryloxy hydroxy soy oils," *Journal of Applied Polymer Science*, Vol. 7, pp. 1853-1855, 1963.
13. Zhu, J.; Chandrashekhara, K.; Flanigan, V.; Kapila, S. "Curing and mechanical characterization of a soy-based epoxy resin system," *Journal of Applied Polymer Science*, Vol. 91, pp. 3513-3518, 2004.
14. Shabeer, A.; Garg, A.; Sundararaman, S.; Chandrashekhara, K.; Flanigan, V.; Kapila, S. "Dynamic mechanical characterization of a soy-based epoxy resin system," *Journal of Applied Polymer Science*, Vol. 98, pp. 1772-1780, 2005.
15. Santosh, D.W.; Jog, J.P. "Effect of modified layered silicate and compatibilizers on the properties of PMP/clay nanocomposites," *Journal of Applied Polymer Science*, Vol. 90, pp. 3233-3238, 2003.
16. Nelson, J.K.; Hu, Y. "Nanocomposite dielectrics-properties and implications," *Journal of Physics D: Applied Physics*, Vol. 38, pp. 213-222, 2005.

Sl. No.	Epon 9500 (gm)	EAS (gm)	LS 56 V (gm)	Clay (gm)
1	25	75	70	0
2	25	75	70	2.5
3	25	75	70	5

**Table 1** Compositions of the soy epoxy anhydride polymer and soy epoxy anhydride polymer-clay nanocomposites

Sample	T <sub>onset</sub> (°C)	T <sub>mid</sub> (°C)	T <sub>end</sub> (°C)	T <sub>g</sub> (°C)	Heat of reaction H (J/g)
Pure resin	79.6	160.3	235.8	14.9	214.8
2.5% clay in resin	75.7	157.7	233.1	13.3	179.9
5% clay in resin	71.6	157.2	230.0	13.0	145.3

**Table 2** Differential scanning calorimetry results

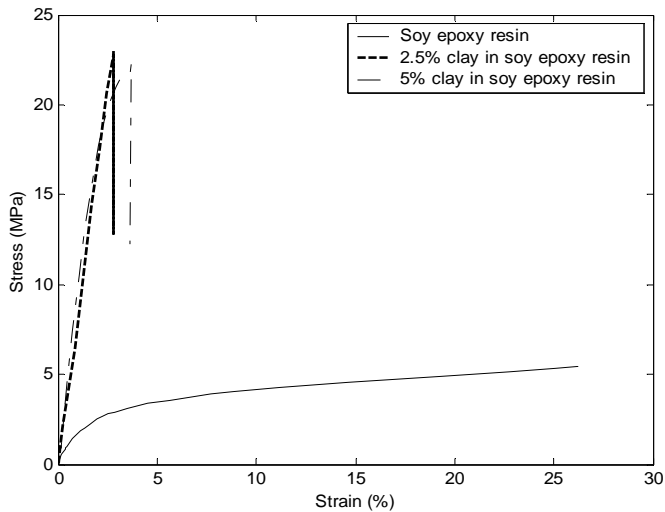


**Figure 1** Tensile stress versus strain curves of soy-based epoxy anhydride polymer-clay nanocomposites

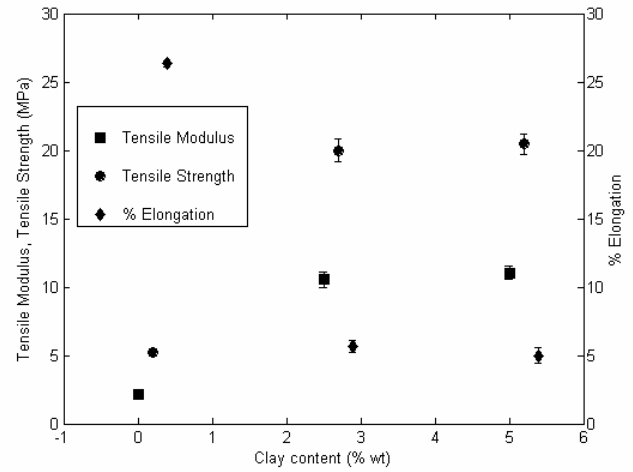


**Figure 2** Mechanical properties of soy-based epoxy anhydride polymer-clay nanocomposites

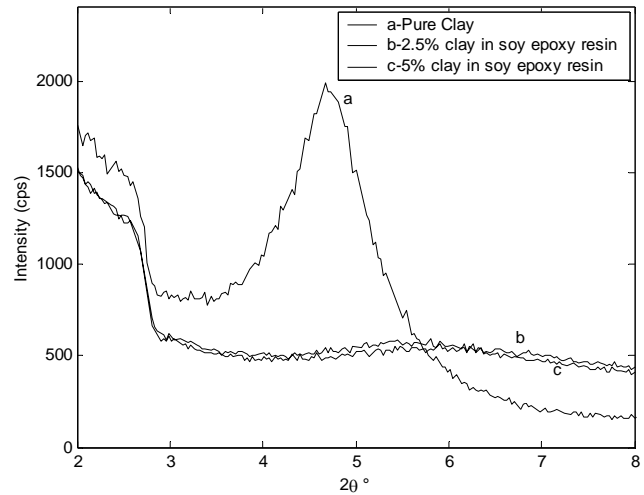


**Figure 3** XRD patterns of pure clay and soy-based epoxy anhydride polymer-clay nanocomposites

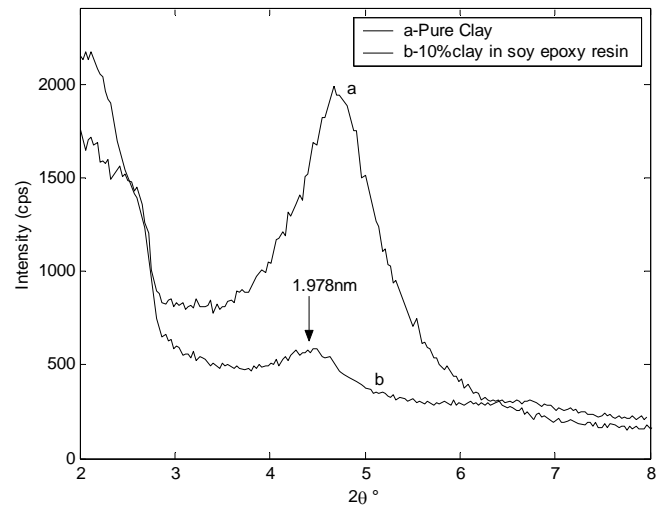


**Figure 4** XRD patterns of uncured soy-based epoxy polymer-clay nanocomposites

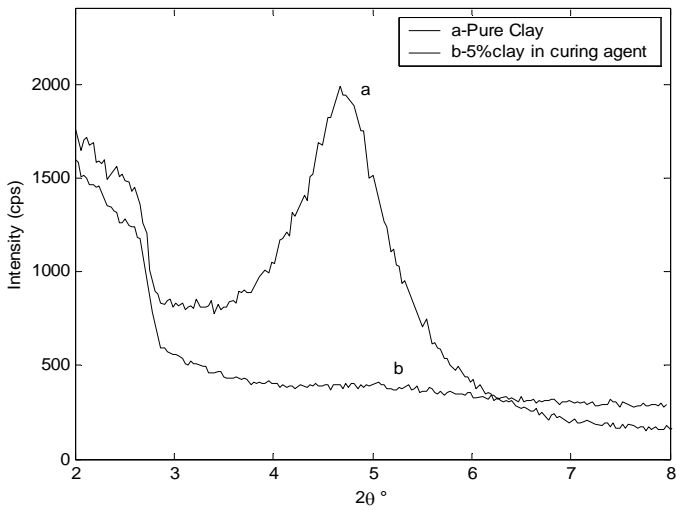


**Figure 5** XRD of pure clay and 5% clay in curing agent

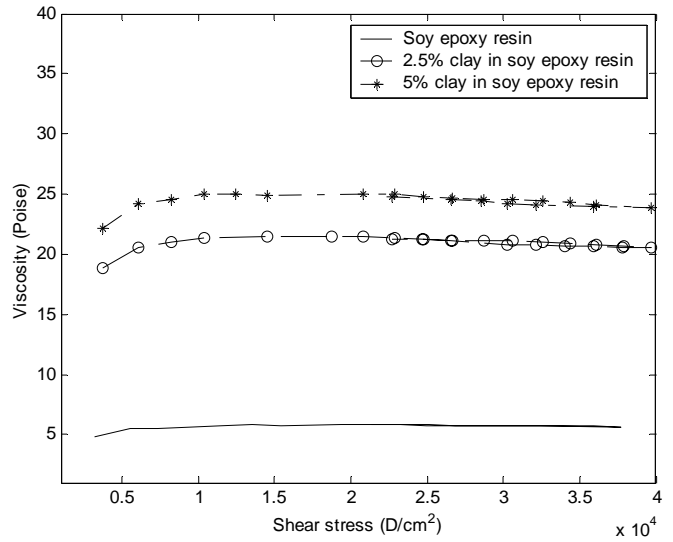


**Figure 8** Viscosity versus shear stress for soy-based epoxy anhydride polymer- clay nanocomposites

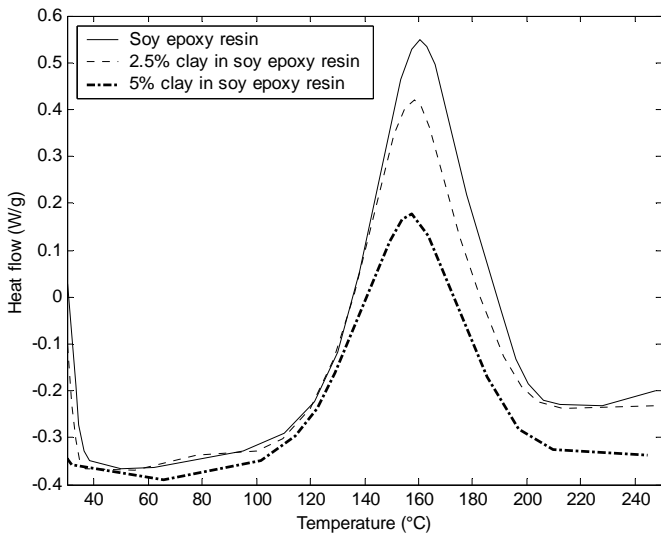


**Figure 6** Dynamic curing curves of soy epoxy anhydride polymer-clay nanocomposites

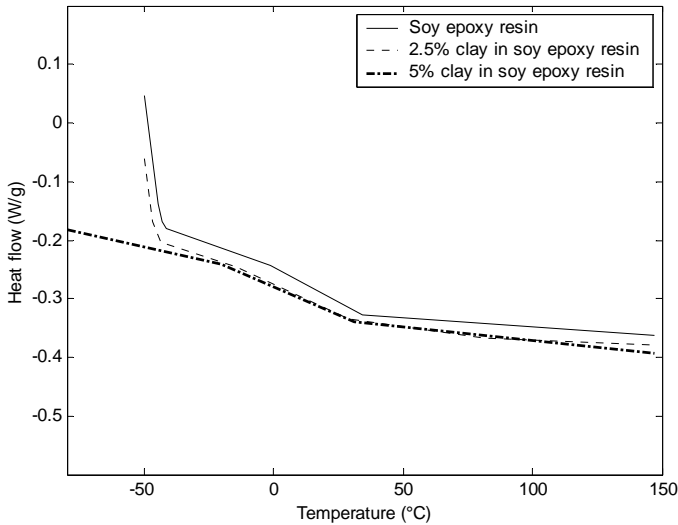


**Figure 7** DSC thermograms showing the glass transition region

**Authors:**  
**A.Shabeer**, Post Doctoral Fellow,  
 Mechanical and Aerospace Engineering,  
 University of Missouri-Rolla

**S. Sundararaman**, Post Doctoral Fellow,  
 Mechanical and Aerospace Engineering,  
 University of Missouri-Rolla

**V.G.K.Menta**, Graduate Student,  
 Mechanical and Aerospace Engineering,  
 University of Missouri-Rolla

**K.Chandrashekhara**, Professor,  
 Mechanical and Aerospace Engineering,  
 University of Missouri-Rolla

**T.Schuman**, Associate Professor,  
 Chemistry,  
 University of Missouri-Rolla